



THE UNIVERSITY *of* EDINBURGH

Edinburgh Research Explorer

## Twisted flow wind tunnel design for yacht aerodynamic studies

**Citation for published version:**

Zasso, A, Fossati, F & Viola, IM 2005, 'Twisted flow wind tunnel design for yacht aerodynamic studies' Paper presented at 4th European and African Conference on Wind Engineering, Prague, Czech Republic, 11/07/05 - 15/07/05, pp. 350-351.

**Link:**

[Link to publication record in Edinburgh Research Explorer](#)

**Document Version:**

Early version, also known as pre-print

**General rights**

Copyright for the publications made accessible via the Edinburgh Research Explorer is retained by the author(s) and / or other copyright owners and it is a condition of accessing these publications that users recognise and abide by the legal requirements associated with these rights.

**Take down policy**

The University of Edinburgh has made every reasonable effort to ensure that Edinburgh Research Explorer content complies with UK legislation. If you believe that the public display of this file breaches copyright please contact [openaccess@ed.ac.uk](mailto:openaccess@ed.ac.uk) providing details, and we will remove access to the work immediately and investigate your claim.



# Twisted Flow Wind Tunnel Design for Yacht Aerodynamic Studies

A. Zasso<sup>1</sup>, F. Fossati<sup>2</sup>, I. Viola<sup>3</sup>

**ABSTRACT:** *This paper presents the research activities carried out in developing a special wind tunnel device (named Twisted Flow Device in the following) aimed at reproducing the variation in the onset wind speed and direction with height as seen by yachts as they sail in the boundary layer above the sea. The concept to produce sheared and twisted flow is to use a series of twisted vanes allowing good flow quality in the model area. The paper shows both computational as well as experimental results measured in the Politecnico di Milano Wind Tunnel.*

## 1 INTRODUCTION

The motion of a yacht sailing in the boundary layer above the sea produces an apparent wind velocity, resulting from the vector addition of the wind and yacht velocities. Since the wind speed increases with height due to the boundary layer phenomena and the boat speed is constant, this means that the apparent wind speed incident onto a yacht also increases with height and, in addition, its direction changes, rotating away from the yacht's heading with increased height (Figure 1, Figure 2). This is a very important topic in wind tunnel testing on sailing yacht scale models, that has to be carefully considered, because the forces developed by the sail plain are due to the apparent wind speed incident onto the sails and the sails shape and trim is strongly related to the apparent wind profile. Therefore, for a proper similitude modelling, the apparent wind velocity sheared and twisted profile has to be reproduced in the wind tunnel for testing stationary models. Moreover, in the same way, it has to be reproduced also using computational fluid dynamics codes.

It should be remembered that there are two main reasons to test sails in a wind tunnel: to provide data for velocity prediction programs (VPPs) and to provide comparative data between different sail designs. As reported elsewhere (Fossati and Diana, 2004; Campbell and Claughton, 1994; Campbell, 1998; Flay and Jackson, 1992), in order to relate changes in sails aerodynamic coefficients to changes in yacht performance, modern yacht design makes use of a VPP, which contains information about the yacht being studied. Based on a hydrodynamic model and an aerodynamic model, VPP calculates yacht performance calculating how long it will take to sail a racecourse under various conditions.

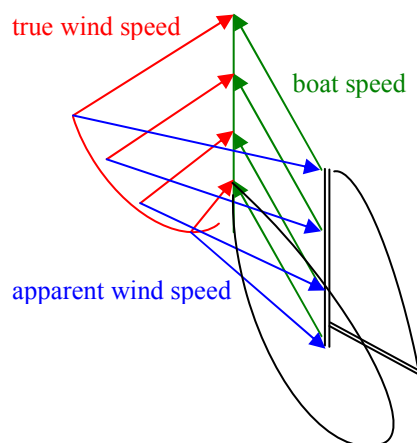


Figure 1 Twisted flow on sailing yacht

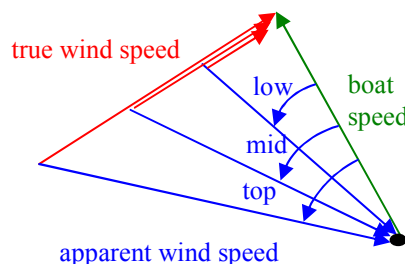


Figure 2 Twisted flow velocity triangles

For this reason, the VPPs aerodynamics models must be as much accurate as possible and hence, a critical role is played by the wind tunnel sail research, in order to provide sail models and coefficients.

While the variation in wind speed with height can be modelled in the wind tunnel using similar procedures as for conventional wind engineering testing, the twisted flow is a more difficult task to deal with for a stationary wind tunnel yacht model,

<sup>1</sup> Prof., Dipartimento di Meccanica, Politecnico di Milano, e-mail [alberto.zasso@polimi.it](mailto:alberto.zasso@polimi.it)

<sup>2</sup> Prof., Wind Tunnel Sailing Yacht Testing Coordinator, Politecnico di Milano, e-mail [fabio.fossati@polimi.it](mailto:fabio.fossati@polimi.it)

<sup>3</sup> Eng, PhD Student, Dipartimento di Meccanica, Politecnico di Milano, e-mail [sail.wt@mecc.polimi.it](mailto:sail.wt@mecc.polimi.it)

because the true and apparent wind speeds are coincident.

Other research groups have considered this problem in the past and different solutions have been attempted. A simple approach is to fire the model along a driving rail at a fixed angle through the boundary layer flow generated in the wind tunnel (Figure 3). Such an approach has been taken by the Nottingham vehicle group (Humphreys and Baker, 1992) and the Politecnico di Milano vehicle group (Bocciolone, Cheli, Corradi, Diana and Tomasini, 2003) in order to obtain force measurements on train and lorries, but many repetitions of each configuration are needed to obtain statistically reliable results.

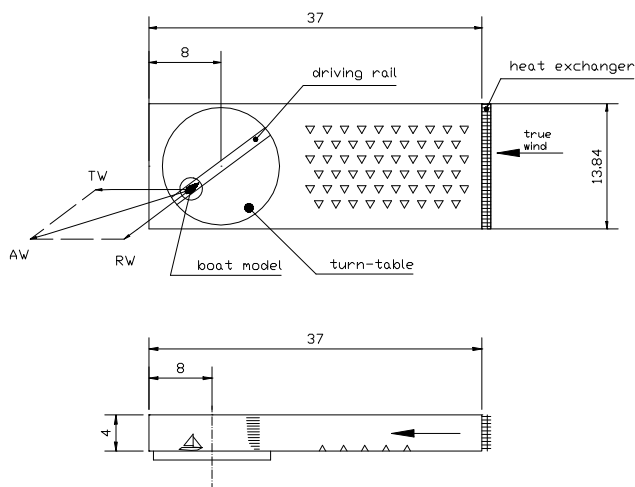


Figure 3 Twisted flow by moving model approach

With reference to yacht testing there is also the practical difficulties associated with the sails flexibility and with the necessary sail trimming during the measure: this provided sufficient reasons for the authors not to pursue this approach.

A rather different approach, was used by the University of Auckland Yacht Research Unit group (Flay, Locke and Mallison, 1996) based on keeping the model stationary and adding a velocity (corresponding to the opposite of the boat speed) to the velocity profile and hence, introduce twist into the onset flow. Conceptually this could be done by building a boundary layer wind tunnel having porous walls, so that an appropriate amount of uniform flow can be introduced through one side porous wall and the same flow rate withdrawn through the other side one.

Another idea is the use of twisted turning vanes at the outlet of a boundary layer wind tunnel: the boundary layer would be used to develop the shear flow and the twisted vanes would be used to develop

appropriate twist based on velocity triangles produced from yacht velocity. Flay, Locke and Mallison (1996) and Flay (1996) quote design activities carried out to realise the twisted flow at the University of Auckland; this facility is an open jet tunnel with a 6 m wide 3 m high test section equipped with a cascade of vertical twisted vanes in order to produce twisted flow.

Politecnico di Milano decided to design and build a new large Wind Tunnel having a very wide spectrum of applications and very high standards of flow quality and testing facilities. The Wind Tunnel is fully operative since September 2001 and since the first year of operations has been fully booked for applications in both fields of Wind Engineering and Aerospace applications.

With reference to sailing yacht design, the usefulness of generating a twisted flow for sailing yacht model testing in Politecnico di Milano Wind Tunnel, emerged during testing activities carried out by the Mechanical Engineering Department of the P.d.M. with Prada syndicate challenger for the America's Cup 2003.

Figure 4 shows an overview of the P.d.M. facility: it's a closed circuit facility in vertical arrangement having two test sections, a 4x4 m high speed low turbulence and a 14x4 m low speed boundary layer test section.

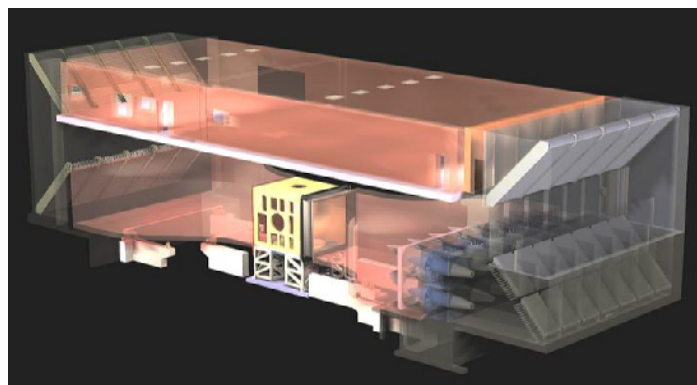


Figure 4: Politecnico di Milano Wind Tunnel the 14 axial fans array (2 m diameter each) is recognizable on the right lower side

The overall wind tunnel characteristics are summarised in Table 1. Peculiarity of the facility is the presence of two test sections of very different characteristics, offering a very wide spectrum of flow conditions, from very low turbulence and high speed in the contracted 4x4 m section ( $I_u < 0.15\%$ ,  $V_{max} = 55$  m/s), to earth boundary layer simulation in the large wind engineering test section. Focusing on the boundary layer test section, its overall size of 36 m length, 14 m width and 4 m height allows for very large-scale wind engineering simulations, as well as

for setting up scale models of very large structures including wide portions of the surrounding territory (Figure 5, Figure 6). The relevant height of the test section and its very large total area (4 m, 56 m<sup>2</sup>) allows for very low blockage effects even if large models were included. The flow quality in smooth flow shows 2% along wind turbulence and  $\pm 3\%$  mean velocity oscillations in the measuring section. A very large 13 m diameter turntable lifted by air-film technology allows for fully automatic rotation of very large and heavy models fitted over it (max load 100.000 N).

The very long low speed section is designed in order to develop a stable boundary layer and the flow conditions are very stable also in terms of temperature due to the presence of a heat exchanger linked in the general control loop of the facility. The Wind Tunnel is operated through an array of 14 axial fans organised in two rows of seven 2x2 m independent cells. 14 independent inverters drive the fans allowing for continuous and independent control of the rotation speed of each fan. This fully computer controlled facility can help in easily obtaining, joined to the traditional spires & roughness technique, a very large range of wind profiles simulating very different flow conditions and very different geometrical scales. The flow conditions were found very stable and a confirmation of that is the very low turbulence level in smooth flow. All the typical various set of spires have been developed in order to simulate the different wind profiles and an original facility has been recently installed allowing for active turbulence control in the low frequency range.

With reference to yacht sail aerodynamic studies, the low speed section allows for testing large scale models (typically 1:10 -1:12 for IACC yacht model) with low blockage effects. Concerning the low-turbulence high-speed section, the large dimensions (4x4 m) and the quite high wind speed (55 m/s) enable to reach quite high Reynolds numbers. Table 1 shows the very low levels of turbulence reached in this section, giving to the facility a very wide spectrum of possible applications. In particular, with reference to yacht studies, the high-speed wind tunnel section allows to develop specific appendage scale model tests typically on 1:2 scale model for IACC class keel and rudder models.

Table 1 Wind tunnel overall characteristics

<b>Politecnico di Milano Wind Tunnel</b>				
<b>Tunnel Overall Dimensions: 50×15×15 [m]</b>				
<b>Maximum Power (Fans only): 1.5 [MW]</b>				
<b>Test Section</b>	<b>Size [m]</b>	<b>Max Speed [m/s]</b>	<b><math>\Delta U/U</math> %</b>	<b>Turb. Int. <math>I_u</math> %</b>
<b>Boundary Layer</b>	<b>14×4</b>	<b>16</b>	<b>&lt; <math>\pm 2</math></b>	<b>&lt; 2</b>
<b>Low Turbulence</b>	<b>4×4</b>	<b>55</b>	<b>&lt; <math>\pm 0.2</math></b>	<b>&lt; 0.2</b>



Figure 5 Wind tunnel vertical section

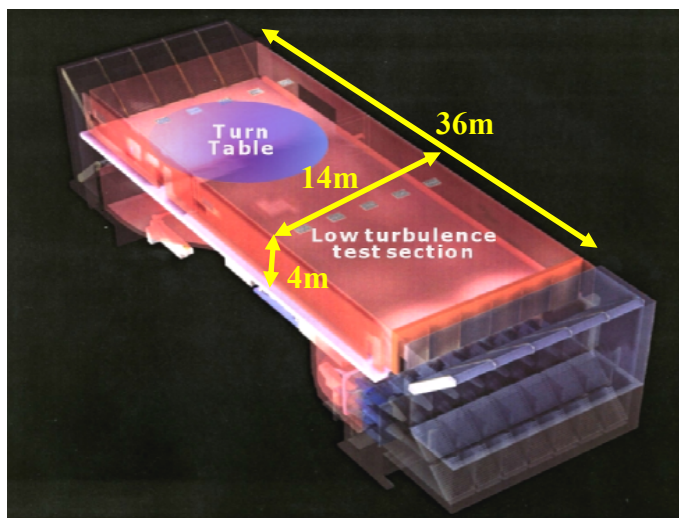


Figure 6 Main dimensions of the low turbulence test section

The Twisted Flow Device concept design had the following basic points:

- To be positioned in the low-speed section
- Guarantee a large area of uniform and controlled twisted flow
- Guarantee persistency of twisted flow state
- Guarantee low turbulence intensity level



The basic idea of the design process is to generate a large-scale vortex with its spin axis aligned with the wind tunnel steady state flow direction, resulting in a twisted flow area in correspondence of the model location.

Moreover, basic design requests were the following:

- easy to adjust
- easy to install/remove
- economical solution both in terms of first installation and running costs

## 2 TWISTED FLOW DEVICE CONCEPT

Figure 7 shows the wind velocity triangle in a horizontal plane, for a yacht sailing upwind and downwind. The apparent wind angle  $\Psi(z)$  variable with the height  $z$ , is defined as the angle between the boat speed  $\vec{V}_b$  and the apparent wind speed  $\vec{V}_a(z)$  (Zasso, Fossati, Viola and Catena, 2004).

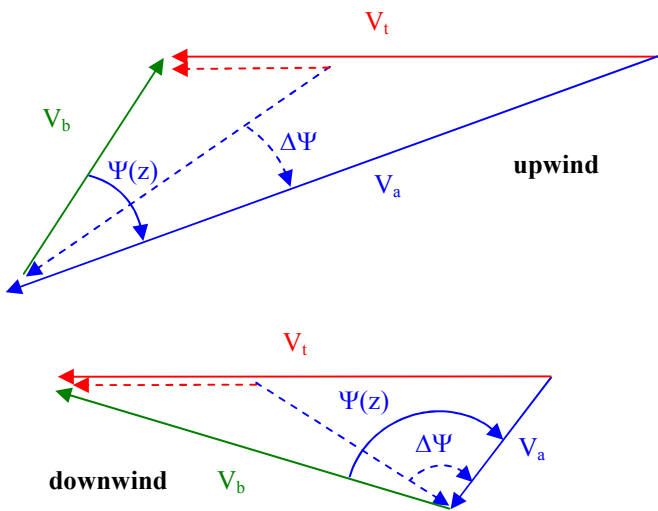


Figure 7 The apparent wind angle  $\Psi(z)$

The apparent wind angle  $\Psi(z)$  increases from zero at water-plane ( $z = 0$ ) until the mast top. By the way, in the wind tunnel, the range of interest is the difference  $\Delta\Psi$ , defined as the difference between the apparent wind angle at the lowest edge of the sail-plan (crosshatch in figure) and the apparent wind angle at the top of the mast.

The wind tunnel tests are referred to a nominal apparent wind angle at the conventional 10 m full-scale height ( $Z_{ref}$ ). As a consequence, the twist

device should generate a deflection angle  $\alpha_T(z)$  defined as:

$$\alpha_T(z) = \Psi(z) - \Psi(z_{ref}) \quad (1)$$

where  $Z_{ref}$  is the reference height.

Hence, the lower part of the flow field is twisted to one side of the wind tunnel and the upper to the other one, allowing for the feasibility of the device and for a reasonable flow rate balance. Figure 8 shows two different examples of  $\alpha_T$  profiles, to be generated in the wind tunnel, respectively for an upwind and a downwind sailing condition.

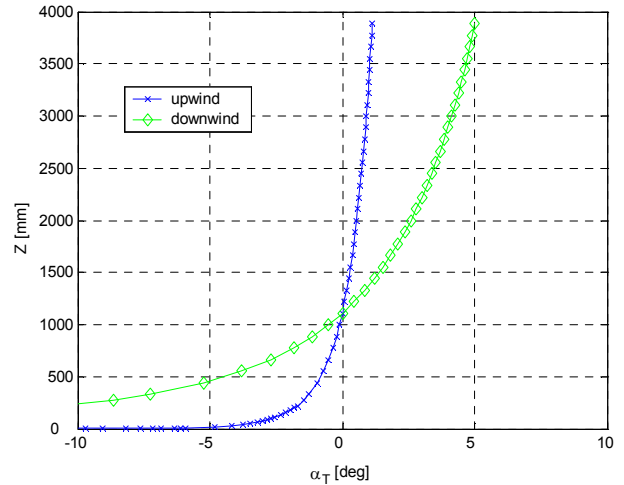


Figure 8 Examples of twist angle  $\alpha_T$  profiles, ( $Z$  values in 1:10 scale)

As a consequence, of the very different  $\alpha_T$  profiles requested, the Twisted Flow Device will be designed in order to allow easy adjustment, keeping constant  $\alpha_T$  regulation at  $Z_{ref}$ .

In general, the twist angle  $\alpha_T$  has a larger vertical gradient in the lower  $z$  range than in the upper one.

Moreover, because the 10 m reference height for a 1:10 – 1:12 scaled model is generally between 800 mm to 1m height, the flow rate twisted to negative angle by the lower part of the vane is significantly less than the flow rate twisted to positive angle by the upper part, if  $Z_{ref}$  is selected as nominal  $\alpha_T = 0$ .

### 2.1 The innovative idea.

The originality of the P.d.M. Twisted Flow Device compared to the other solutions is the central positioning of the device, not occupying the entire tunnel section. In fact, the role of the Twisted Flow Device is just to turn left the lower part and to turn right the upper part of the flow. The side flow not passing through the vanes is allowed to move vertically balancing the flow rate.

The fundamental role of the side flows, having vertical velocity component in the device correct functioning, is clearly shown by the following 2D numerical simulation results.

Figure 9 upper, shows the concept path lines, represented by the local twist angle in Figure 9 lower.

The Twisted Flow Device turns the flow pattern (colouring in blue the path lines), but due to the strong wall effect, the flow is quickly straighten back (green), showing inefficient functioning of a 2D concept. The colours are referred to the twist angle defined as:

$$\alpha_T = \arctan\left(\frac{V_y}{V_x}\right) \frac{180}{\pi} \quad (2)$$

where  $V_x$  is the longitudinal component and  $V_y$  the transversal component of the flow velocity.

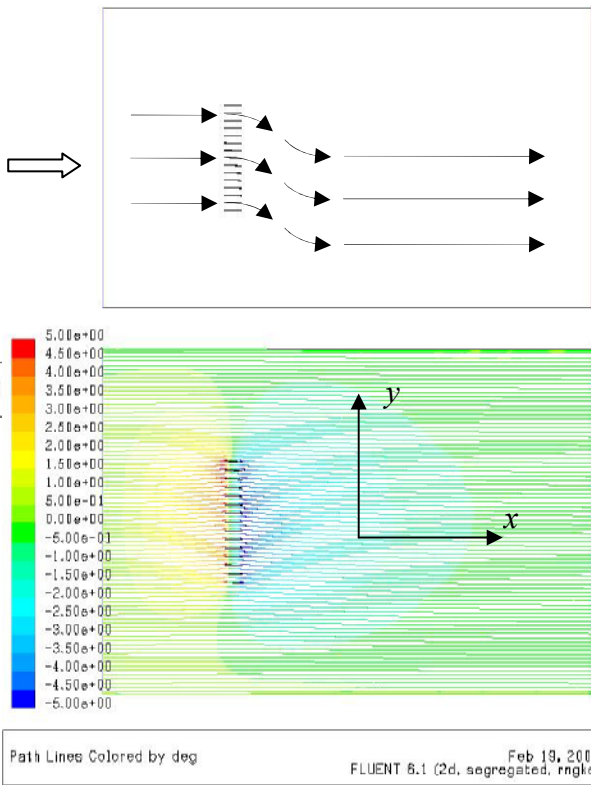


Figure 9 The 2D CFD simulation of a horizontal section of the wind tunnel does not consider the vertical component of velocity. Hence, the presence of the wall straighten the flow

On the other hand, a 3D simulation shows the correct behaviour of the Twisted Flow Device. Figure 10 shows the whole tunnel chamber, where a large longitudinal vortex is generated.

This large-scale vortex guaranties the persistency of twisted flow state behind the device.

Note that the colour of each path lines does not change any more along the chamber, differently by

the 2D case, which means that the Twisted Flow Device imprints a permanent angle  $\alpha_T$  to the flow.

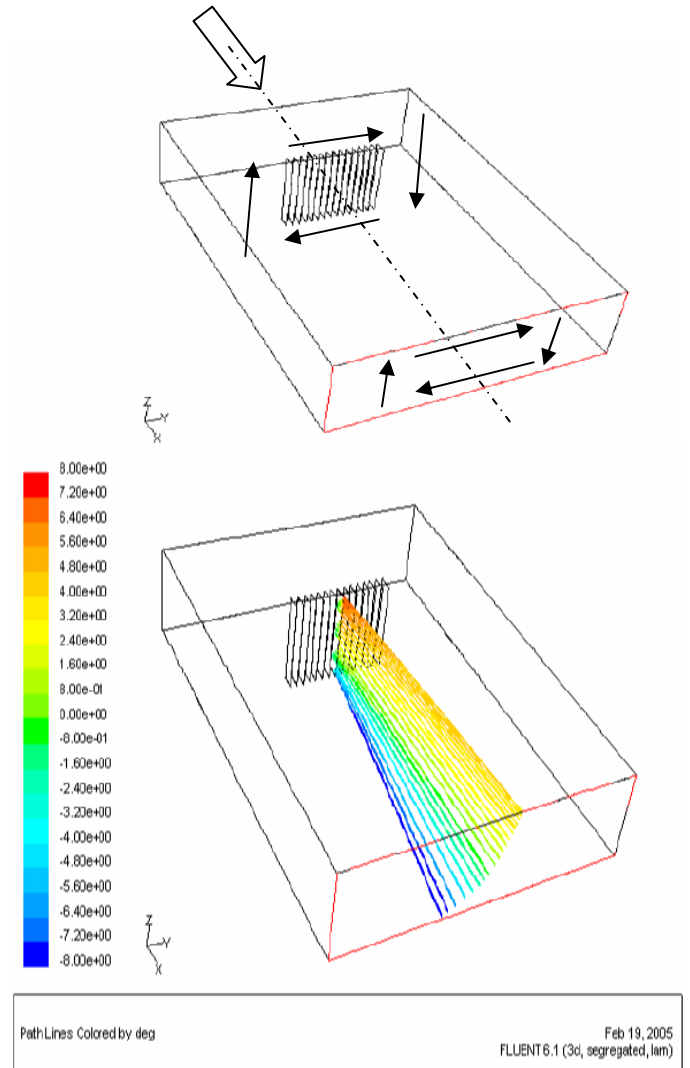


Figure 10 The 3D CFD simulation of the wind tunnel shows the permanent longitudinal vortex induced by the Twisted Flow Device

## 2.2 Feasibility study

A basic experimental study has been initially performed in the 1:9 scale model of the Wind Tunnel Facility (Figure 11).

The pilot tunnel was reconfigured with a pilot device realised with a composite carbon fibre frame equipped with a cascade of 16 vanes set to a reasonable twist angle of  $\pm 10^\circ$ , giving a component of the flow in the positive y direction at the bottom and a negative y direction at the top (see Figure 12). Then the flow was surveyed with a multi-hole probe attached to a computer controlled traversing rig in order to have a velocity map both in magnitude and angle (Zasso, Fossati, Viola and Catena, 2004).

The measures confirmed the feasibility of the twisted turning vanes concept. As an example, Figure 13 shows velocity map measured behind the pilot device in the test section.



Figure 11 Politecnico di Milano Wind Tunnel  
1:9 scale model

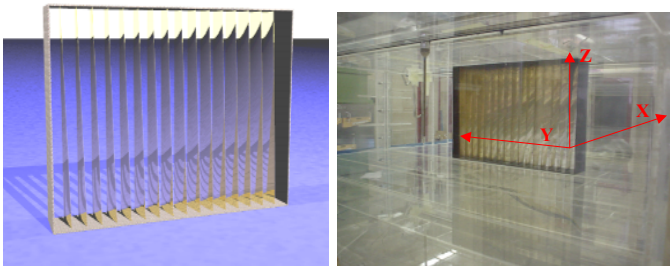


Figure 12 The pilot Twisted Flow Device rendering  
and a picture of it in the 1:9 scale wind tunnel

### 3 FULL SCALE DEVICE DESIGN

The Twisted Flow Device was designed on the basic idea of 15 flat plate turning vanes polycarbonate array having a chord of 70 cm and lateral spacing of 35 cm. The vanes span extends from floor to roof. The leading edges were held straight into the flow by horizontal stainless strip. Horizontal wires were attached to the trailing edges at six heights and screw-bottles were used to twist all the trailing edges in parallel in such a way to adjust the twist angle of the flow (Figure 14).

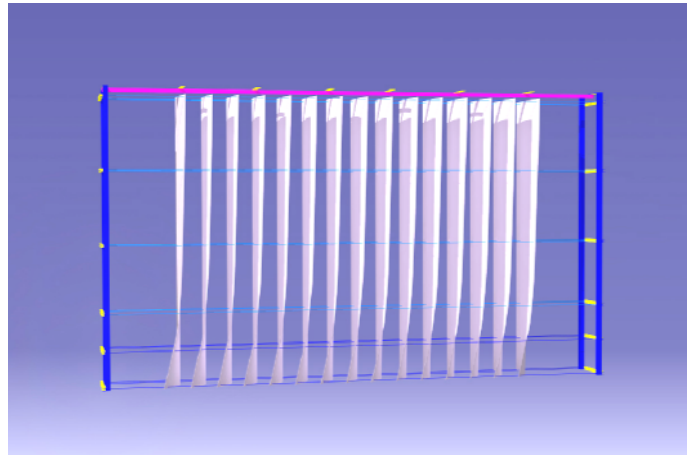


Figure 14 The full-scale Twisted Flow Device rendering

Figure 15 shows the full-scale device installed inside the wind tunnel during a yacht model test session, while Figure 16 shows a detail of the screw-bottles fixed to the lateral frame.

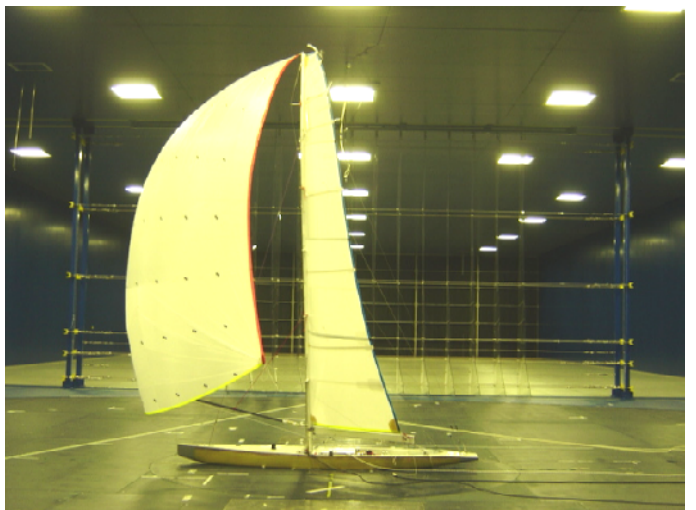


Figure 15 The full-scale Twisted Vanes Device  
in Politecnico di Milano Wind Tunnel

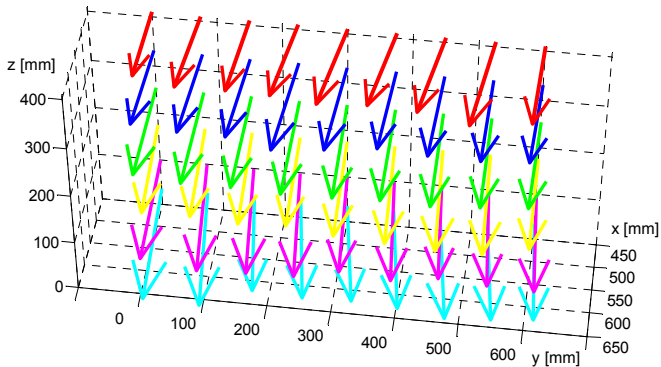


Figure 13 Avg. velocity vectors map  
measured in the test section

In view of the foregoing promising results, the Twisted Flow Device option was developed into the full-scale wind tunnel.



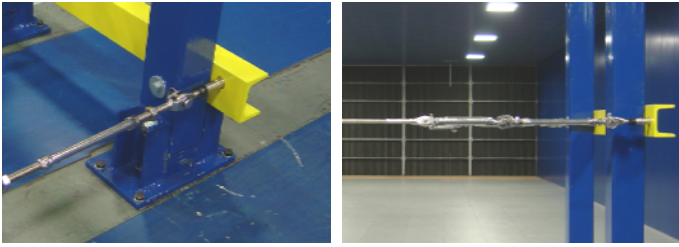


Figure 16 screw-bottles details

The top of each vane can move inside a track fixed to the wind tunnel roof in such a way that, when control cables are slacked, all vanes can be packed and removed from the wind tunnel using a specially designed tool (see Figure 17 and Figure 18) allowing for very quick installation and dismounting.



Figure 17 Track on the wind tunnel roof

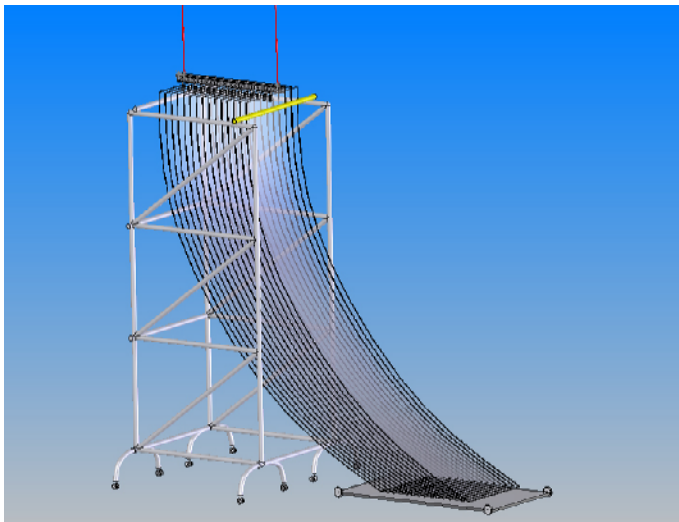


Figure 18 Installation device tool

The authors have assessed a special devoted CAD-CAE procedure in order to manage technological, structural and fluid-dynamic topics of the device design (Figure 19).

In particular, the input control cable displacement, chosen in order to realise a desired twist of the flow, automatically generates in CATIA environment a 3D parametric model of the Twisted Flow Device and its structure.

Then a structural analysis can be directly performed using finite element method in ABAQUS environment in order to evaluate forces in the steel cables and relevant stresses both in the vanes and in

the frame structure. Moreover, the 3D model is automatically meshed by GAMBIT thanks to a pre-built parametric journal file. Finally, the CFD analysis of the flow generated by the Twisted Flow Device onto the model area, inside the wind tunnel, can be performed.

An optimization iterative procedure is finally controlled by an EXCEL spread sheet defining the new configuration to be processed in order to match the target twisted flow parameters.

This design loop has been used in order to evaluate the full-scale device concept design.

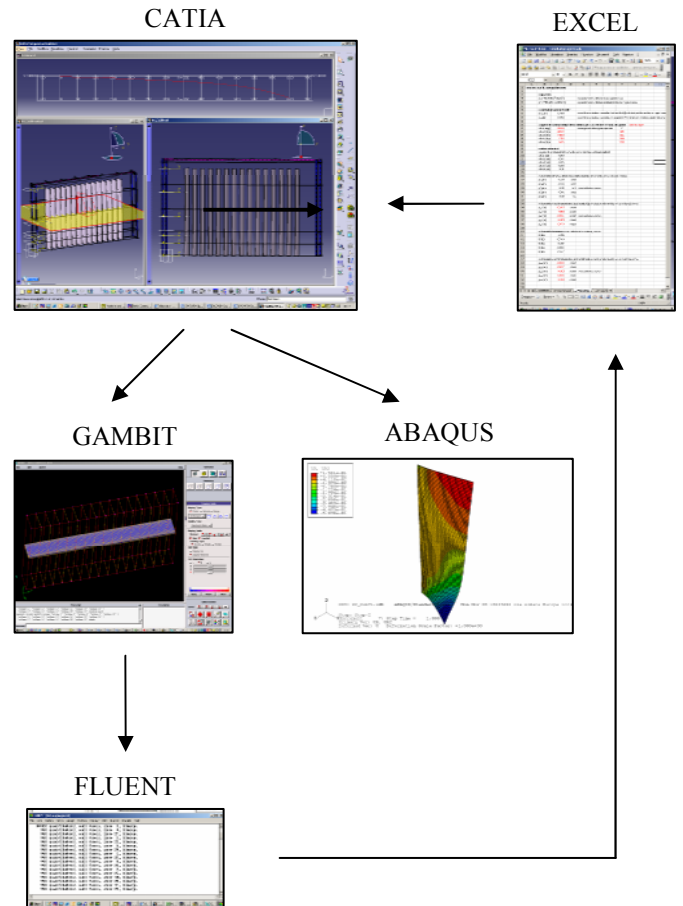


Figure 19 CAD-CAE design procedure

#### 4 TWISTED FLOW DEVICE MOCK-UP

In order to perform a validation of the CAD-CAE design procedure and to have a preliminary evaluation of the fluid-dynamic behaviour of the vane design, a device mock-up has been realised.

In particular, a three vanes mock-up was built with three different vane materials in order to check different damping and viscoelastic properties (Figure 20). In fact, viscoelastic properties have strong relationship with stress level trend and capability to guarantee the proper vane shape requested by the



desired twist profile, while damping properties are strictly related to possible flow induced vibrations.

More in details, each vane of the mock-up has been equipped by means of load cell; than long term measures have been performed in order to check the loads relaxing of control cables (Figure 21).

At the same time, the vane shape has been checked to: as an example in Figure 22 static deflection at different vane chord positions is reported with respect to initial load step, after 12 hours and after 72 hours for the chosen final solution in polycarbonate.

Figure 23 shows the mock-up placed in the wind tunnel with a multi-hole probe during a check up of downstream flow properties.

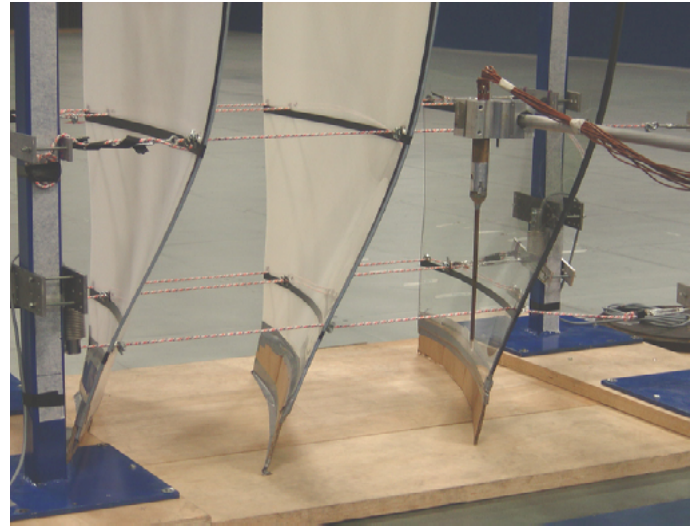


Figure 23 Downstream flow properties check

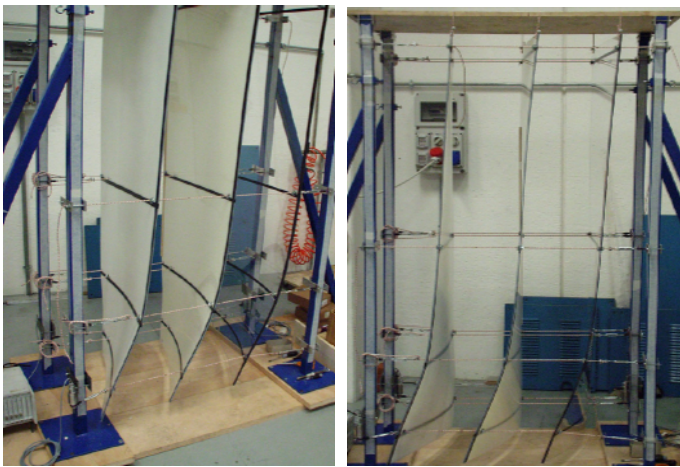


Figure 20 Mock-up

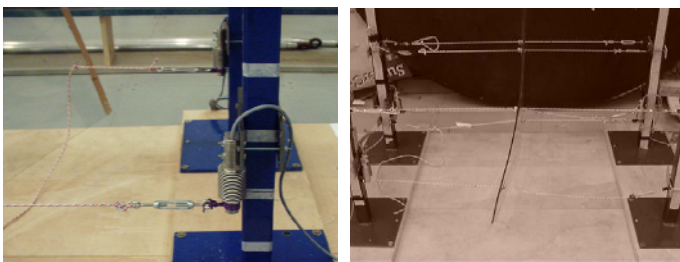


Figure 21 Load cells of the vanes control cable

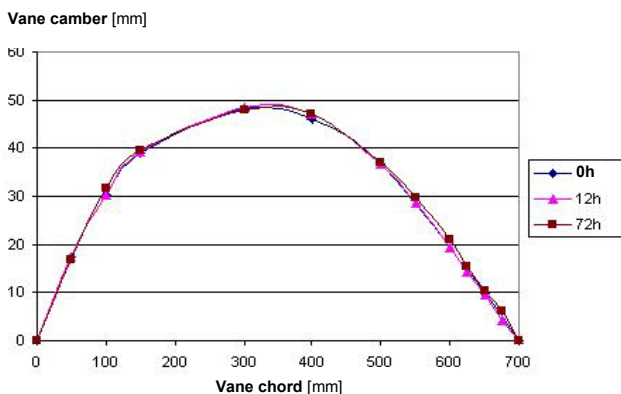


Figure 22 Flat plate vane camber after 12 and 72 hours

## 5 RANS CODE ANALYSIS

### 5.1 The bi-dimensional computation

The local fluid dynamics of the vanes cascade can be correctly investigate through 2D CFD analysis.

At this purpose, the design process over described generates an updated meshed at any change in the main geometrical dimensions of the Twisted Flow Device, allowing to perform a sensitivity investigation on the vanes dimensions and offset.

Figure 24 shows the mesh of the 2D domain. The meshed surface is 20 m long and as large as the tunnel (14 m), meshed with 250.000 cells.

A general triangular mesh is used in the far domain correlating the cell dimension with the twist angle and adopting between the vanes a regular grid of quadrilateral mesh elements, helping the computation of the boundary layer (Figure 24 in the middle).

The optimised solution showed always attached flow on the vanes curved surface in the whole range of twist angle required.

Figure 24 (the lowest) shows the vorticity  $\xi = \vec{\nabla} \times \vec{V}$  around three vanes in the definitive proportion and offset at an average  $\alpha_T$ .

The flow is completely attached and the wake fades rapidly, confirming the adequate choice of the flat plate solution for the turning vanes.

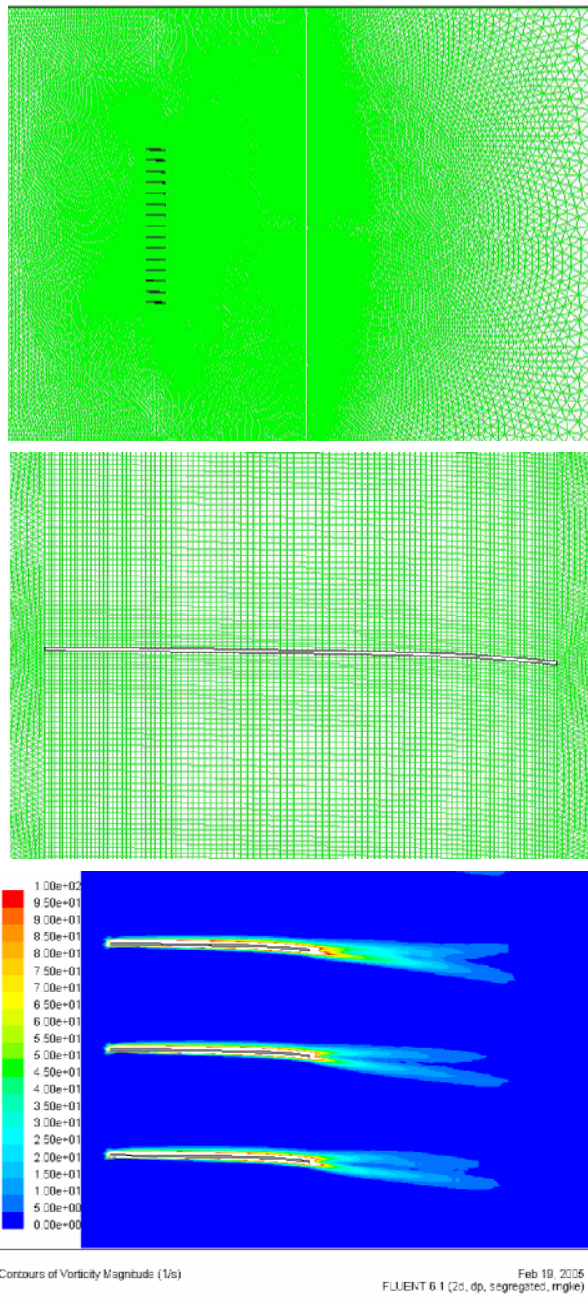


Figure 24 2D domain mesh of the wind vanes cascade

The steady analysis applies a “RNG  $\kappa - \varepsilon$ ” turbulence model (renormalization group theory), which enhances accuracy for swirling flow and provides an analytically-derived differential formula for effective viscosity in low-Reynolds numbers. “Standard wall function” (Launder and Spalding, 1974) used with a  $y^+ = 50$ , warrants the correct boundary layer treatment.

Boundary conditions are the flow velocity in the left hand edge of the figure above, and the static pressure on the right hand edge.

## 5.2 The three-dimensional computation

As previously mentioned, the 3D computation has been used to understand the flow structure and to predict the correct vanes geometry allowing to obtain the requested profile in the volume surrounding the yacht model.

Several different geometric configurations of the vanes have been studied to find out the correlation between the vanes trailing edge angle profile and the twisted flow around the yacht model.

Figure 25 shows the 3D volume. The meshed domain has the same section of the wind tunnel (14 m wide, 3.84 m height), 20 m long and is meshed with more than 2 millions cells.

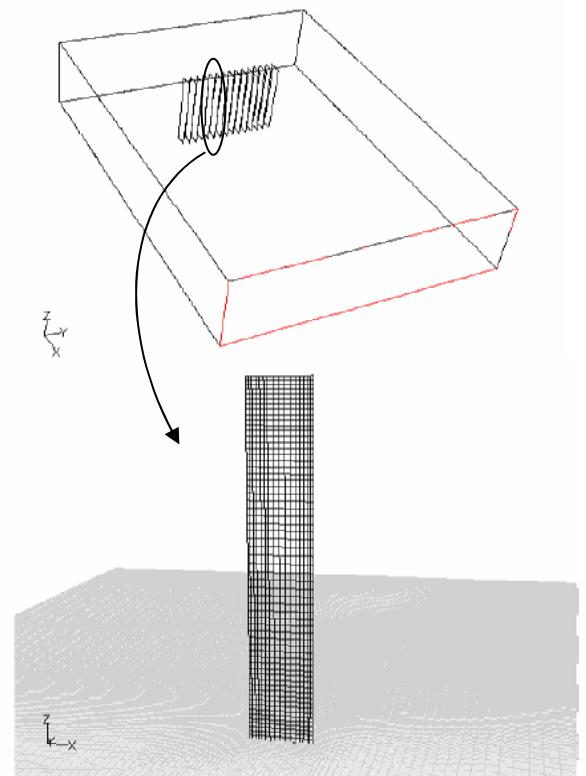


Figure 25 3D volume mesh of the wind vanes cascade

No large mesh elements are allowed in any domain region being the large longitudinal vortex developed in all the wind tunnel simulated domain. The correct simulation of the large vortex required minimization of the numerical diffusion and, as a consequence, as a first help, a regular fine grid of hexahedral mesh elements has been used, possibly with two faces perpendicular to the flow velocity.

Figure 25 shows the vane face mesh.



On the other hand, being required high computation velocity in order to investigate a wide range of geometrical vanes configurations, an acceptable compromise has been chosen between the maximum number of cells and diffusion problem.

The flat plate vanes are aerodynamic profiles with thin wakes, as shown by the 2D numerical computation. Therefore, a non-viscous behaviour could manage the flow field and an “in-viscid” model has been adopted, saving a large amount of cells close to the wall and computational time.

In any case, “adapted mesh” and “viscous models” has been successively processed to validate the in-viscid results.

Second order discretization scheme has been selected for pressure and momentum equations increasing solution accuracy.

As for the 2D computation, the physical problem does not need any un-steady analysis.

Figure 26 shows the vortex generation afterwards the Twisted Flow Device. Colours on four successive transversal sections, illustrate the twist angle defined as above (Equation 2). On the left and right side of all the four sections, there is no twist angle, but a vertical component of wind speed grows.

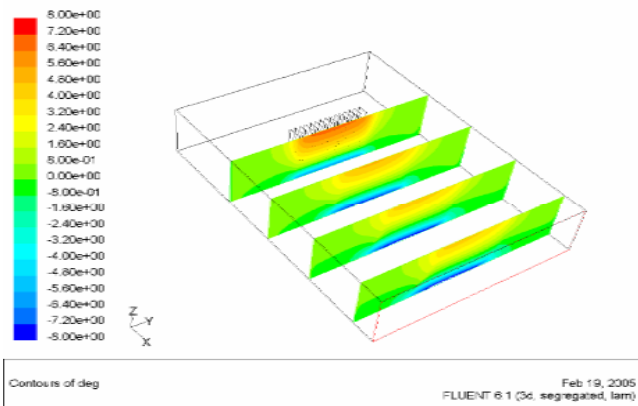


Figure 26 3D results: twist angle  $\alpha_T$  persistency in transversal sections (showing the large longitudinal vortex generation)

Figure 27 shows a horizontal section at 2 m height from the floor, coloured by the magnitude of the vertical component of wind velocity, clearly shown as positive and negative at the left and right sides. On the other hand, no vertical velocity is found in the central stripe of the section behind the Twisted Flow Device.

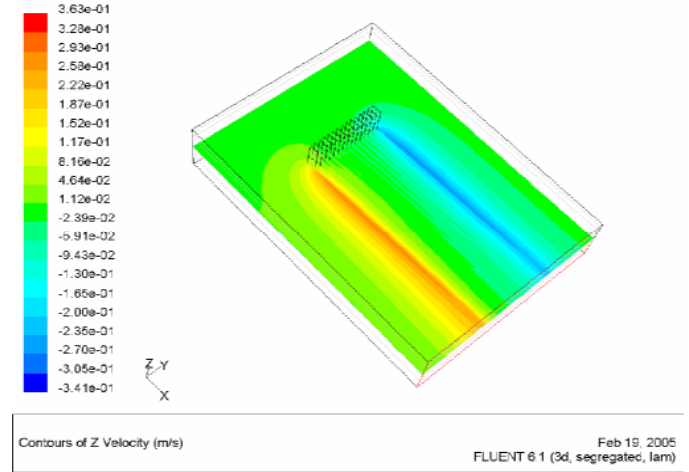


Figure 27 3D results: z velocity contour

Figure 28 shows four horizontal sections at increasing height, coloured by the twist angle. It is possible to appreciate the evolution of the twist angle along the tunnel: on the lowest section at 0.5 m height from the tunnel floor, the flow is deflected to the left by the device, increasing the twist angle moving away from the vanes (from azure to blue colour). In the second section, at 1 m height from the floor, the vanes are almost straight and the flow has no twist anywhere. On the third and fourth sections, at 2 m and 3 m height, the device deflects the flow on the right. The twist angle shows a negligible decrease moving away from the vanes (from darker to brighter orange colour).

The increase of the twist angle in the lower section and the decrease in the upper sections as function of x, could be explained as follows analysing longitudinal vertical flow trend.

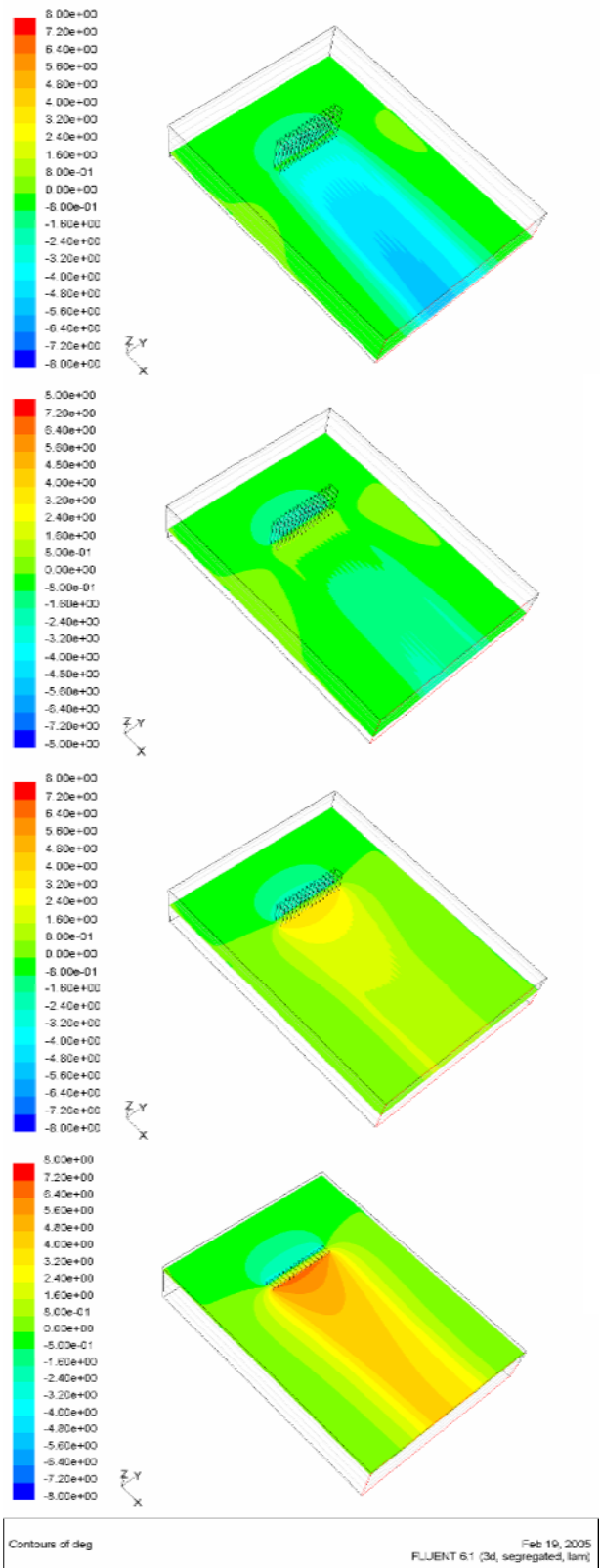


Figure 28 3D results: twist angle  $\alpha_T$  horizontal section patch

In particular, Figure 29 shows, three vertical sections coloured by the twist angle, in which the diffusion of the *vertical twist angle gradient* is well visible. In fact, as shown above (Figure 8), the gradient is much bigger close to the floor of the tunnel than in the upper part.

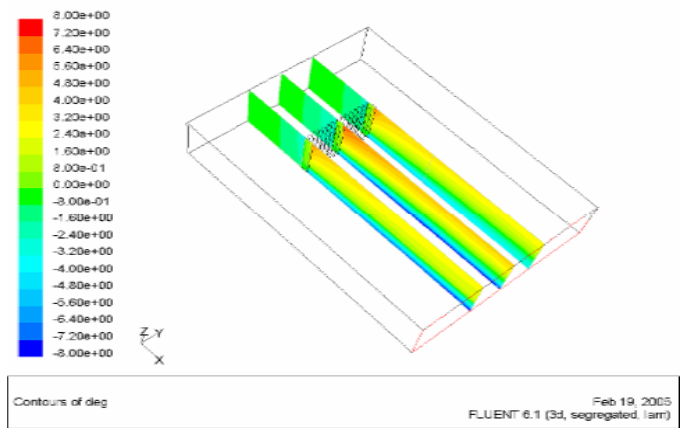


Figure 29 3D results: twist angle  $\alpha_T$  vertical section patch

## 6 EXPERIMENTAL ANALYSIS

### 6.1 The Twisted Flow Device test

The fundamental characteristic of the flow generated by the full-scale device has been tested, both in terms of twist angle and average wind velocity profile (Figure 30), in order to compare the experimental data with the numerical results, setting up the device in the same configuration selected for the numerical simulations.

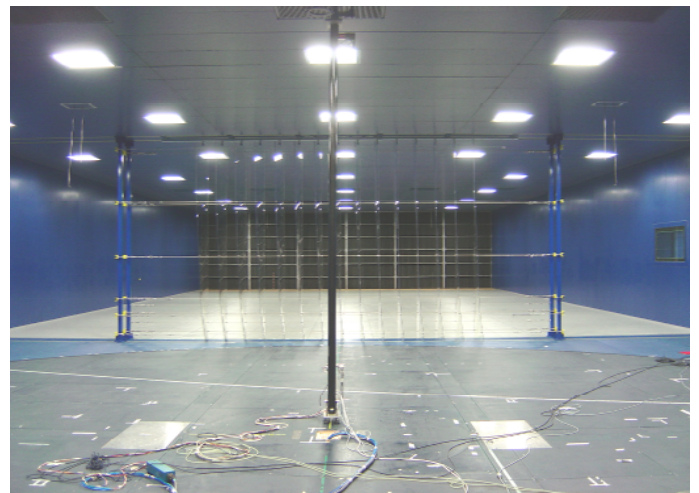


Figure 30 Experimental twisted flow mapping

The flow characteristics in the horizontal plane have been measured through a cross-wire anemometer, a multi-hole probe and a pitot tube.

Figure 30 shows the computer control traversing rig arranged for vertical profiles and positioned downwind the twisted flow device, at the turn-table centre, i.e. at the location corresponding to the tested yacht model.

In previous measured campaign, a larger region of the wind tunnel has been mapped ahead of the



Twisted Flow Device, in order to monitor the incoming flow characteristic.

Further characterisation of the directional properties of the incoming flow has been performed with empty wind tunnel configuration (no Twisted Flow Device installed) through a symmetric wing profile positioned at the turntable centre, measuring the cross-flow lift. The alignment of the wing profile giving zero lift has been compared with the geometrical wind tunnel axis confirming excellent alignment of the flow and has also been used for selecting the angular zero reference of the instrumentation.

Figure 31 shows experimental data compared to the numerical results in terms of twist angle  $\alpha_T$  versus wind tunnel height. Three vertical profiles are shown in correspondence to the test section centre ( $Y = 0$ ) and two sides positions ( $Y = -1350$  mm,  $Y = +1340$  mm), corresponding to the typical 1:10 scaled yacht model volume.

As can be seen, the acquired data confirmed the uniformity of the twisted flow in the volume typically spanned by the sailplane, as well as the correct behaviour of the Twisted Flow Device and the persistency of the twisted flow. In fact, the experimental twist angle profile shows values in the same order or even larger, than the numerical predicted ones.

It should be noted that experimental values evidence a strong persistency of the twisted flow profile, confirming, in the experimental data at high Reynolds numbers, more optimistic results than in the numerical simulation. At this purpose, a work in progress activity is aimed at a deeper understanding of differences shown by the numerical and experimental results.

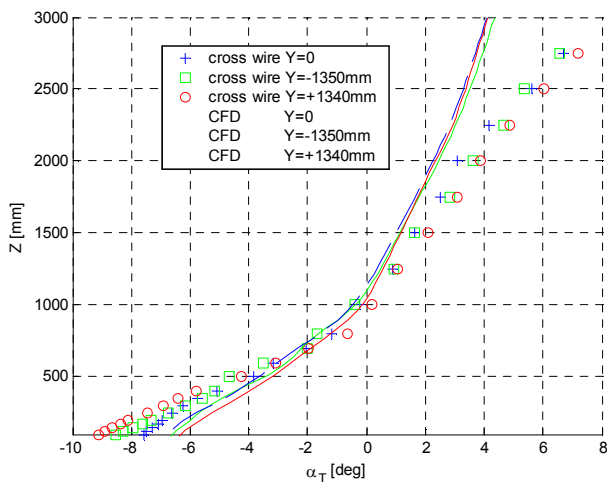


Figure 31 Comparison of twist angle  $\alpha_T$  experimental and numerical results

The previously described behaviour of the Twisted Flow Device didn't show critical dependence on the average incoming flow wind profile, nor on the averaged wind velocity value, at least in the typical ranges of sailing yacht tests.

As an example, Figure 32 shows two wind profiles measured at turntable centre, corresponding to the typical sea breeze and land breeze conditions, normalized at the same 800mm reference height (scaled model), in correspondence of which no difference has been shown by the corresponding twist angle profile  $\alpha_T$  (Figure 31).

The velocity profile is referred to the average wind velocity in the horizontal plane:

$$|V| = \sqrt{V_x^2 + V_y^2} \quad (3)$$

The smooth adjustment of the velocity profiles has been obtained by means of a proper control of the fan array speed distribution, maintaining at the same time always a quite constant level of flow turbulence intensity.

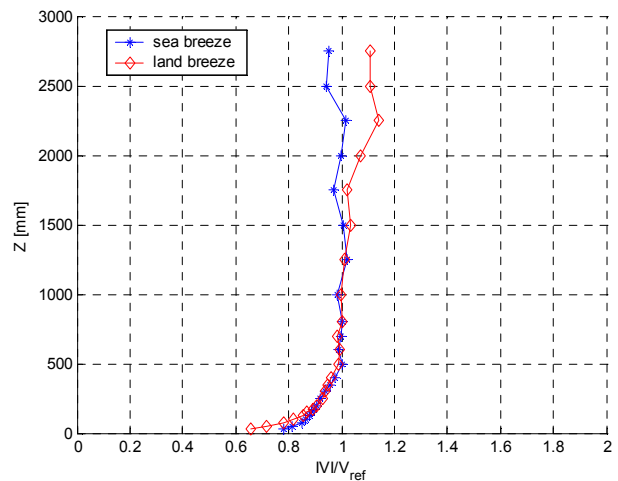


Figure 32 wind velocity profiles

Figure 33 shows the along wind ( $I_u$ ) and transversal ( $I_v$ ) horizontal turbulence index measured as a function of the wind tunnel height relevant to wind profiles of Figure 32. It is clearly shown that for  $z > 0.5m$ , holds  $I_u \cong 2\%$ ,  $I_v \cong 2\%$ , confirming that the Twisted Flow Device doesn't change significantly the wind tunnel turbulence index in the range of fans regulations parameters over mentioned.

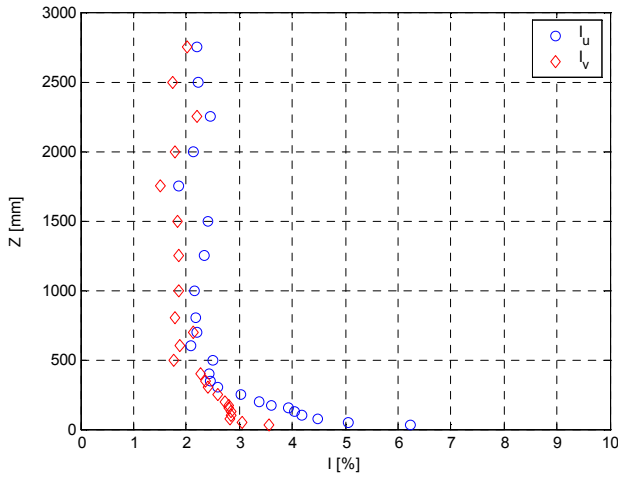


Figure 33 Measured turbulence index profiles

### 6.2 The Twisted Flow Device features

Several different configurations of the Twisted Flow Device have been tested spanning the most significant configurations required by the different boat sailing course shown in Figure 8.

As an example Figure 34, shows three twist profiles, for upwind, downwind and intermediate conditions.

Figure 35 shows several different velocity profiles, obtained through regulations of the upper and lower row fans array.

It should be reminded that an increasing level of turbulence should be necessarily faced by the configurations having large gradient of average wind speed.

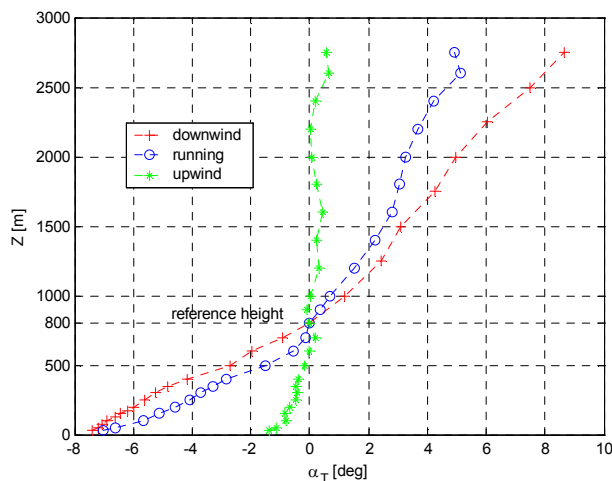


Figure 34 Measured twist angle profiles

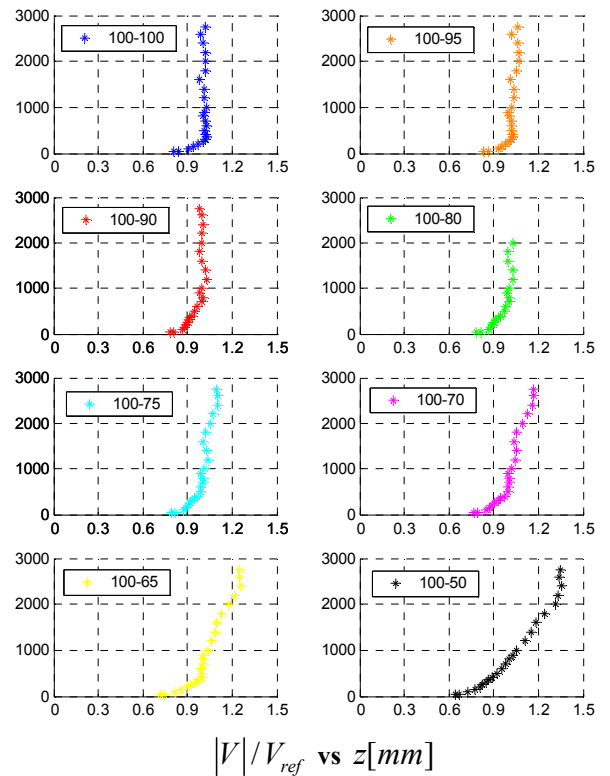


Figure 35 Measured average wind velocity profiles

## 7 CONCLUSIONS

In this paper the design process for a full-scale Twisted Flow Device, allowing for sailing yacht testing in the wind tunnel has been described.

Twisted Flow Device based on the concept of a twisted vanes array, simply placed in the centre of the flow stream, revealed optimal behaviour of the generated flow in a large volume of the test section as required by the 1:10 yacht scaled model size.

This has been achieved by means of a successful design procedure, based on a CAD-CAE process linked to a CFD code.

The realized device allowed to obtain different twist angle target profiles without need of large extra deflection of the vanes, which could lead to a critical aerodynamic working condition of the flat plate profiles.

The persistency of the obtained twist angle is adequate to the large-scale model size and low turbulence intensity level can be achieved.

The realized device permits an easy adjustment of the vanes, has a light structural design allowing for an easy and quick installation and removing procedure, leading to an economical advantage from both running and first installation costs.

## 8 REFERENCES

- F. Fossati, G. Diana – L'ottimizzazione delle Prestazioni Attraverso la Ricerca in Galleria del Vento – *seminario La Ricerca nello Yacht Design* - Milano 2003
- F. Fossati, M. Belloli, A. Zasso - Prove in galleria del vento su modelli di imbarcazioni a vela - *XII Convegno Nazionale di Ingegneria del Vento* - Milano 2002
- J. M. C. Campbell, A. R. Cloughton – Wind Tunnel Testing of Sailing Yacht Rigs – *13<sup>th</sup> HISV Symposium* – Amsterdam 1994
- J. M. C. Campbell – The Performance of Offwind Sails Obtained from Wind Tunnel Tests – *RINA International Conference on Modern Yacht* –1998
- Bocciolone M., Cheli F., Corradi R., Diana G. Tomasini G - Wind tunnel tests for the identification of the aerodynamic forces on rail vehicles - *11th ICWE – International Conference on Wind Engineering* – Lubbock, Texas - June 2003
- H. Hansen, P. Jackson, K. Hochkirch - Comparison of Wind Tunnel and full-scale Aerodynamic sail force measurements. - *High Performance Yacht Design Conference* - Auckland, 4-6 Dicembre 2002
- Kevin R. Cooper - The Wind Tunnel simulation of Wind Turbulence for surface vehicle testing. - *Journal of Wind Engineering and industrial Aerodynamics*, 38 (1991) 71-81 - Elsevier Science Publishers B.V., Amsterdam
- R. I. Harris - Some Further thoughts on the Spectrum of Gustiness in Strong Winds. - *Journal of Wind Engineering and industrial Aerodynamics*, 33 (1990) 461-477 - Elsevier Science Publishers B.V., Amsterdam
- R. G. J. Flay, N. J. Locke, G.D. Mallison - Model test of Twisted flow Wind Tunnel designs for testing yacht sails. - *Journal of Wind Engineering and industrial Aerodynamics*, 63 (1996) 155-169 - Elsevier Science Publishers B.V., Amsterdam
- R. G. J. Flay, P. S. Jackson - Flow Simulation for Wind-Tunnel Studies of Sail Aerodynamics. - *Journal of Wind Engineering and industrial Aerodynamics*, 41-44 (1992) 2703-2714 - Elsevier Science Publishers B.V., Amsterdam
- R. G. J. Flay - A twisted flow wind tunnel for testing yacht sails. - *Journal of Wind Engineering and industrial Aerodynamics*, 63 (1996) 171-182 - Elsevier Science Publishers B.V., Amsterdam
- R. G. J. Flay, R.J. Andrews - A wind tunnel/full scale comparison of the wind flow over Auckland City. - *Journal of Wind Engineering and industrial Aerodynamics*, 54/55 (1995) 151-161 - Elsevier Science Publishers B.V., Amsterdam
- K. L. Hedges, P. J. Richards, G. D. Mallison - Computer modelling of downwind sails. - *Journal of Wind Engineering and industrial Aerodynamics*, 63 (1996) 95-110 - Elsevier Science Publishers B.V., Amsterdam
- R. G. J. Flay, I. J. Vuletich - Development of a wind tunnel test facility for yacht aerodynamic studies. - *Journal of Wind Engineering and industrial Aerodynamics*, 58 (1995) 231-258 - Elsevier Science Publishers B.V., Amsterdam
- A. Zasso, F. Fossati, I. M. Viola, P. Catena - Analisi delle caratteristiche del flusso per prove di imbarcazioni a vela in Galleria del Vento su modelli in scala – *8<sup>o</sup> italian conference on wind engineering IN-VENTO-2004*, Reggio Calabria
- B.E. Launder and D.B. Spalding; The Numerical Computation of Turbulent Flows; *Computer Methods in Applied Mechanics and Engineering*, 3:269-289, 1974